Letter

Electrochemically induced metallization of NaCl: Use of the main component of salt as a cost-effective electrode material for sodium-ion batteries

Iqra Moeez, Hee-Dae Lim, Jae-Ho Park, Hun-Gi Jung, and Kyung Yoon Chung

ACS Energy Lett., **Just Accepted Manuscript** • DOI: 10.1021/acsenergylett.9b01118 • Publication Date (Web): 11 Jul 2019

Electrochemically induced metallization of NaCl: Use of the main component of salt as a cost-effective electrode material for sodium-ion batteries

Iqra Moeez[1, 2], Hee-Dae Lim[1, 2], Jae-Ho Park[1, 3], Hun-Gi Jung[1, 2] and Kyung Yoon Chung[1, 2*]

[1] Center for Energy Storage Research, Korea Institute of Science and technology, Hwarang-ro 14-gil 5, Seongbuk-gu, Seoul 02792, Republic of Korea

[2] Division of Energy and Environment Technology, KIST School, Korea University of Science and Technology, Seoul 02792, Republic of Korea

[3] Department of Materials Science and Engineering, Korea University, Seoul 02841, Republic of Korea

ABSTRACT: Sodium chloride (NaCl), a typical stoichiometric ionic compounds, breaks all of the basic rules of chemistry at high pressures and can form new metallic compounds with different stoichiometries of Na_xCl at x>1. However, the electrochemical phase transition of NaCl from an insulating state to a metallic state without pressurization has not been achieved to date. In this study, we first demonstrate that nonmetallic NaCl can be transformed to a metallic compound through an electrochemical activation process. Subsequently, the activated NaCl electrode was shown to intercalate/deintercalate sodium-ions into the structure, with a discharge capacity of 267 mAh/g by reversibly accommodating 0.6 Na-ions. We believe that this method may represent a new approach for designing inexpensive electrode materials using the main component of table/sea salt for sodium-ion batteries (NIBs). In addition, these results will contribute to the development of low-cost and sustainable rechargeable batteries that can be operated at a room temperature.

Cationic sodium (Na^+) and anionic chlorine (Cl^-) form NaCl under ambient conditions with strong ionic bonds at a 1:1 stoichiometry due to the large electronegative differences between the atoms. NaCl is a typical nonmetallic and brittle material that exists as a highly compressible solid and has been widely used for pressure calibration due to its elastic properties.[1] Inspired by these fascinating properties, considerable efforts have been made to understand sodium chloride systems. The chemistry of NaCl under ambient conditions is well-understood; however, the abnormal condition of extremely high pressure can change the local bonding nature of NaCl, leading to different electronic and mechanical properties, as well as chemical reactivity.[2-8] Recently, Zhang *et al.* demonstrated that various Na_mCl_n phases with different stoichiometries, such as Na_3Cl, Na_2Cl, $NaCl_3$, and $NaCl_7$, can be induced under different pressure conditions in the presence of excess sodium and chlorine atoms.[2] With theoretical predictions and diamond anvil cell experiments, these researchers found that these compounds are thermodynamically stable by maintaining unusual bonding structures and electronic properties. The researchers also predicted that sodium-enriched subchlorides (i.e., Na_mCl) can conduct electricity along the layers of the structures. For example, the layered structure of Na_3Cl can be represented as a sequence of layers ([NaCl][Na][Na][NaCl][Na][Na]• • •), where the pure sodium layer conducts electricity.[2] Hence, under pressure, NaCl systems are capable of turning into a diverse array of metallic compounds with the potential for new practical applications.

The metallization of alkali halides (such as NaF) can also be performed by substituting an electron with a halogen-ion (F^-) in the presence of excess metal ions (Na^+). This transition is similar to a type of crystallographic defect in which an anion vacancy in the crystal is filled with one or more unpaired electrons. These defects, in the form of vacancies, would provide activation sites for the phase transition and significantly reduce the pressure required for the B1 to B2 phase transition.[9,10] Devani *et al.* also investigated the effects of vacancies on the pressure required for B1- to B2-KCl phase transitions and reported that the phase transition can be initiated at a defect site with the B2-phase spreading throughout the entire crystal.[11] While the pressure required for the B1 to B2 phase transition decreased as the number of vacancies increased. It should be noted that the transitions of theses alkali halides have only been achieved under high pressure conditions, which requires high cost and is not applicable in practical applications.

On the basis of material resources, sodium-ion batteries (NIBs) are regarded as an alternative battery technology for large-scale sustainable energy storage.[1,2] Currently, the major challenges are to find new cost-effective electrode materials for NIBs with high volumetric energy density. For the practical use of NIBs to meet the tough challenges, a number of intercalation cathode materials have been investigated, such as layered oxides ($NaxMO_2$), polyanions ($NaMXO_4$), fluoropolyanions ($NaMXO_4F$) and pyrophosphates ($Na_2MP_2O_7$).[13-16] Manganese

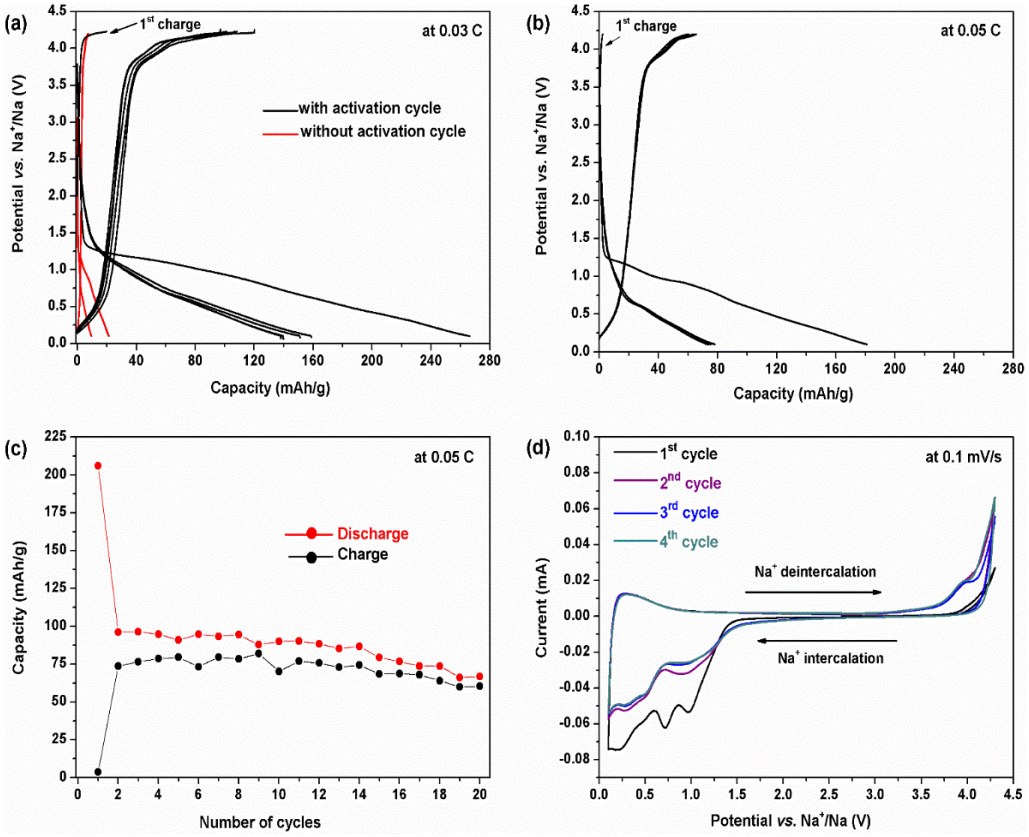

Figure 1. Galvano-static profiles of NaCl electrode. (a) Sodium intercalation and deintercalation process through the NaCl structure with and without activation cycle at 0.03 C-rate. (b) Charge and discharge profile of the activated NaCl electrode at 0.05 C-rate. (c) Galvano-static cyclic performance of NaCl up to 20 cycles. (d) Cyclic voltammetry curve of the NaCl electrode measured at 0.1 mV/s in a sodium half-cell.

and iron are earth abundant elements, and NIBs with manganese/iron-based materials, such as P2-$Na_{0.67}Fe_{0.5}Mn_{0.5}O_2$, may provide a solution for meeting the difficult challenges involved in achieving economically sustainable energy development.[17,18] However, it will be more beneficial if more cost-effective and eco-friendly materials are used for the electrode material. Sodium salts, such as NaCl, the main component of table salt (or sea salt), is notably inexpensive and abundant in sea water and can be a candidate as an electrode material for NIBs. Inspired by previous work on metallization of NaCl under high pressure, we report a simple activation process to make NaCl electrochemically active and to use it as an electrode material for NIBs. Metallization of NaCl is achieved by electrochemically inducing defects in the crystal structure. This strategy enables nonmetallic NaCl to be used as a metallic-electrode material for NIBs. To make this compound electrochemically active, vacancies are intentionally induced through the precharge step, resulting in the partial phase transition from B1- to B2-NaCl. Further, during electrochemical discharge process, sodium-ions are intercalated into the compound during electrochemical discharge process. When sodium-ions move back into the NaCl structure during the discharge process, the electrochemically active B2-NaCl phase can effectively accommodate sodium-ions and form a sodium-rich compound (Na_xCl, x >1). It is noteworthy that this metallic NaCl material can reversibly intercalate/deintercalate sodium-ions with a high discharge capacity of 267 mAh/g. Additionally, we cycled the NaCl electrodes up to 20 cycles in the voltage range between 0.1 and 4.23 V at a 0.05 C-rate. Various analyses by combining *ex-situ* and *in-situ* X-ray diffraction (XRD) techniques were used to investigate the chemical composition of ions and the changes in the NaCl structure upon sodium intercalation/deintercalation cycling. This research provides insights into a new chemistry as an alternative to conventional NIB applications.

The metallization of NaCl is a key process to electrochemically activate it for reversible cycling. The cyclic performance (Figure 1) of metallic NaCl electrodes, which had been precharged to form the active B2-phase, show the successful intercalation/deintercalation of sodium-ions at 0.03 and 0.05 C-rates, as shown in Figure 1a and 1b, respectively. To electrochemically activate B1-NaCl (i.e., the nonmetallic compound), which shows negligible discharge/charge capacity (Figure 1a), the activation process of a first charging step is required. When a high potential over 4.0 V is applied during the charge process, free sodium-ions are generated from the bond breaking of B1-NaCl (i.e., 0.04 Na^+ calculated based on a capacity). This process not only make defects (in the form of ion vacancies) in the solid ionic structure but also triggers the

phase transition from B1- to B2-NaCl, resulting in the formation of a Na-deficient phase of

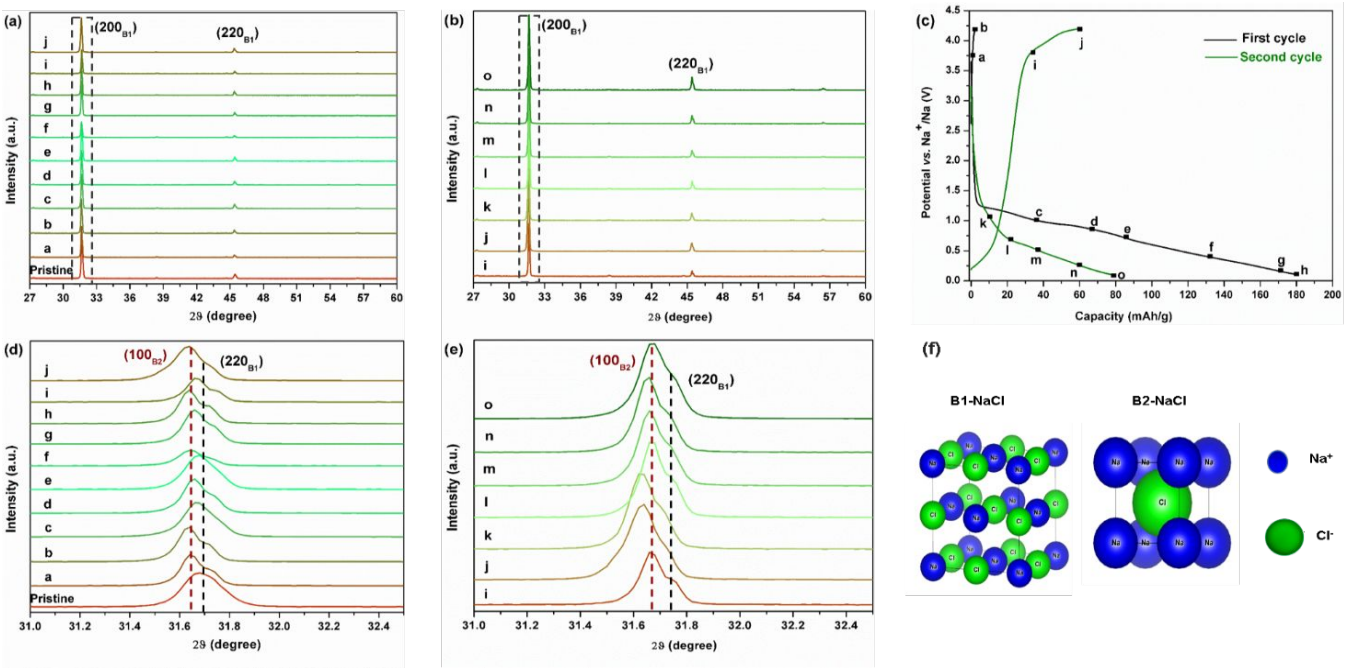

Figure 2. Structure transition of B1-, B2- and metallic-NaCl. *Ex-situ* XRD patterns of sodium chloride electrode for the (a) 1st and (b) 2nd cycles at (c) discrete voltage depths during charge and discharge processes. (d, e) B1 to B2 phase transition and effect of sodium-ion intercalation/deintercalation on the peak position shown in (a) and (b) between 31° and 32.6°. (f) Crystal structure of B1-NaCl (face centered cubic structure with six fold coordination) and B2-NaCl (like CsCl: body centered cubic structure with eight fold coordination).

Na_xCl (x<1). During the discharge process, the sodium-ions can be inserted into the B2-NaCl host and occupy the newly formed vacancies in the crystal structure. Interestingly, NaCl can be oversodiated beyond the original state of Na_1Cl, and the host forms a new sodium-enriched NaCl compound, i.e., $Na_{1.6}Cl$ (Equation 1). Then, the sodium-ions are successfully deintercalated from the metallic-NaCl electrode during the charge process (second charge). High discharge capacities of 267 mAh/g (i.e., intercalation of 0.6 Na^+ ions) and 180 mAh/g (i.e., intercalation of 0.4 Na^+ ions) at 0.03 and 0.05 C-rates, respectively, are achieved, where the theoretical capacity of NaCl is 458 mAh/g. Additionally, the cyclic performance of NaCl at 0.05 C (Figure 1c) confirms that the sodium de/intercalation in B2-NaCl structure can be reversibly operated. However, the contribution of the acetylene black (Supplementary Figure 1b) is excluded in the calculation of specific capacity of NaCl electrode. 20 % of acetylene black in the NaCl electrode, attributes ~65 mAh/g, which corresponds to 24.3% from the total capacity of NaCl electrode (Figure 1a), based on the capacity of AB/PVDF: 90/10 electrode. Achieving the first application of the main component of table salt (or sea salt), NaCl, which is one of the least expensive and most abundant materials on earth, as an electrode material would be meaningful. The irreversible capacity loss in the initial cycle is due to the consumption of sodium-ions trapped in the new metallic phase or the formation of solid electrolyte interface (SEI) at the electrode surface, as previously reported.[19-23] Cyclic voltammetry (CV) curves (Figure 1d) matches well with that of a charge and discharge profile, as shown in Figure 1a and 1b.

While one dominant anodic peak at 4.2 V is observed for the activation step, three cathodic peaks are observed during the first intercalation process of sodium-ions. The first cathodic peak at 1.0 V disappeared during subsequent cycles, which corresponds to the formation of the SEI films on the surface of the NaCl electrode. The other peaks below 1.0 V correspond to the formation of the Na/NaCl interface and further phase transition during the intercalation of sodium-ions into the layers of the B1- and B2-NaCl structures. In the second cycle, two anodic peaks at approximately 0.3 V and 3.9 V reflect the reversible de/intercalation of sodium-ions. After the second cycle, the current peaks became stable, which shows that the sodium-ions can be reversibly intercalated/deintercalated in the B2-NaCl structure. The effect of activation process is also studied by using electrochemical impedance spectroscopy (EIS). EIS of the NaCl electrode before and after the activation process (Supplementary Figure 2) reflects that the electric conductivity of the electrolyte and electrodes is enhanced after the activation process. The EIS study confirmed that B1 to B2 phase transition improves NaCl electrochemical, electrical, and ionic conductivity. Naeemullah *et al.* also observed that the band gap energy is improved after the B1 to B2 phase transition with enhanced electronic conductivity.[24]

To investigate structural changes of B1- and B2-NaCl upon cycling, *ex-situ* (Figure 2) and *in-situ* (XRD) (Figure 3) were carried out using a half-cell configuration with sodium metal as the counter electrode. *Ex-situ* XRDs were measured at different depths of charge and discharge during the first and second cycles at 0.05 C (Figure 2a-c). The *ex-situ* XRD patterns at 3.75 V (step a) and 4.23 V (step b) demonstrate the phase transition

from B1- to B2-NaCl during the first charge process (steps a and b, described in Figure 2a and 2d). The dominant $(100)_{B2}$ peak at 31.65º after the precharge step indicates the formation of B2-NaCl phase. During both the first and second discharge pro processes (c-h and k-o), the $(100)_{B2}$ peak shifts to a higher degree, while the peak shifts to a lower degree after the second charge (step i and j in Figure 2b and 2e). Shifting of peaks during intercalation of sodium-ions reflects the volume changes of B1- and B2-NaCl due to the Na-Na and Na-Cl interactions (Figure 2f). Bu *et al.* explained that metallic-Na_xCl (x>1) has four distinct bonds in the system: (a) Na–Cl ionic bonds joining two adjacent Na and Cl ions, (b) ionic bonds of Na–Na with two distinct electro-negativities, (c) Na–Na metallic bonds connecting two Na atoms with the same or different electro-negativities, and (d) Cl–Cl covalent bonds.[25] These bonds are the main reason for the gradual breaking of the partial ionic bonds and the formation of Na/NaCl interfaces during the intercalation/deintercalation processes of sodium-ions.[25] This electrochemical transition of crystal structure is similar to the phase transitions, which have only been achieved under high pressure as previously reported.[2-8] As a reference, the structural behavior without the activation cycle (precharge step) was also studied using *ex-situ* XRD analysis (Note. S1). The appearance of sodium fluoride (NaF) peak during the discharge process reflects consumptions of sodium-ions to form SEI layer on the electrode that are dissolved at the end of charge process (Supplementary Figure 3).To investigate the phase transition of NaCl during electrochemical cycling, *in-situ* XRD was conducted as shown in Figure 3(a-f). At the end of first charge (Figure 3a and 3b), a small shoulder peak on 44.8°appears, demonstrating the formation of B2-NaCl $(110)_{B2}$; direct proof for the phase transition from B1- to B2-NaCl. After the activation process in first charge, structural changes during the first discharge is shown in Figure 3c and 3d. A new dominant peak at approximately 55.2° corresponds to B2-NaCl at 1.0 V, which was not identified in the first charge process. This peak signals the presence of intercalated sodium-ions in the Na-Cl ionic bonding. The intercalated sodium-ions can induce partial breaking of Na-Cl ionic bond, which could facilitate successive B1 to B2 phase transitions. It is also worth noting that another shoulder peak at 31.1° at a potential near 0.6 V (Figure 3d) was observed which matched with the sodium metal phase with space group of P63/mmc (PDF card No. 9008507). Compared to normal metallic sodium (a=b=3.7670 Å and c=6.1540), the lattice constants of the intercalated sodium for the fully discharged electrode have a lower a-lattice parameter and a higher c-lattice parameter, *i.e.,* a=b=3.7139 Å and c=6.3262 Å. The increased c-lattice would be attributed to a repulsive effect between ionically bonded sodium in the NaCl structure (Na^+) and the intercalated sodium (metallic Na) between the NaCl layers. As explained by Zhang *et al.*, for Na_xCl at x>1, sodium atoms form a 2D metallic array between the layer of B2-NaCl structures.[2] The lattice constants of fully discharged electrode (Figure 3c) are a=b=c=5.6213 Å for B1-NaCl and a=b=c=2.8597 Å for the B2-NaCl. The origin of this volume reduction in NaCl structure during intercalation of sodium-ions can be understood by comparing the coordination spheres of Cl^- anion in B2-NaCl. The environment of Cl^- anion is similar to CsCl structure, where two units have anion-anion coordination (Figure 2f). Zhang *et al*. showed that the intercalation of sodium-ions can be deposited between the layers of B2-NaCl structure.[2] Therefore, the replacement of one anion by a cation to form cation-anion coordination can reduce the distance between them, which results in the reduction of volume for the metallic-NaCl structure. The volume reduction mechanism is also confirmed by *ex-situ* XRDs studied after 5th and 10th cycles (Supplementary Figure 4). The lattice constants for the fully charged electrode (Figure 3e and 3f) are increased to a=b=c=5.6398 Å for B1-NaCl and a=b=c=2.8612 Å for the B2-NaCl, which means that partial absence of sodium-ions in the host structure leads to the relaxation in Na-Na and Na-Cl bonds. For further verification of B1-B2 phase transition and sodium intercalation into the structure, high resolution *ex-situ* XRDs for the NaCl pristine and cycled electrode, are measured that also support this *in-situ* XRD study (Supplementary Figure 5). In addition, to get a better understanding of the behavior of NaCl electrode upon intercalation-deintercalation of sodium-ions, we carried out galvano-static intermittent titration technique (GITT) experiment that allows characterizing the material in

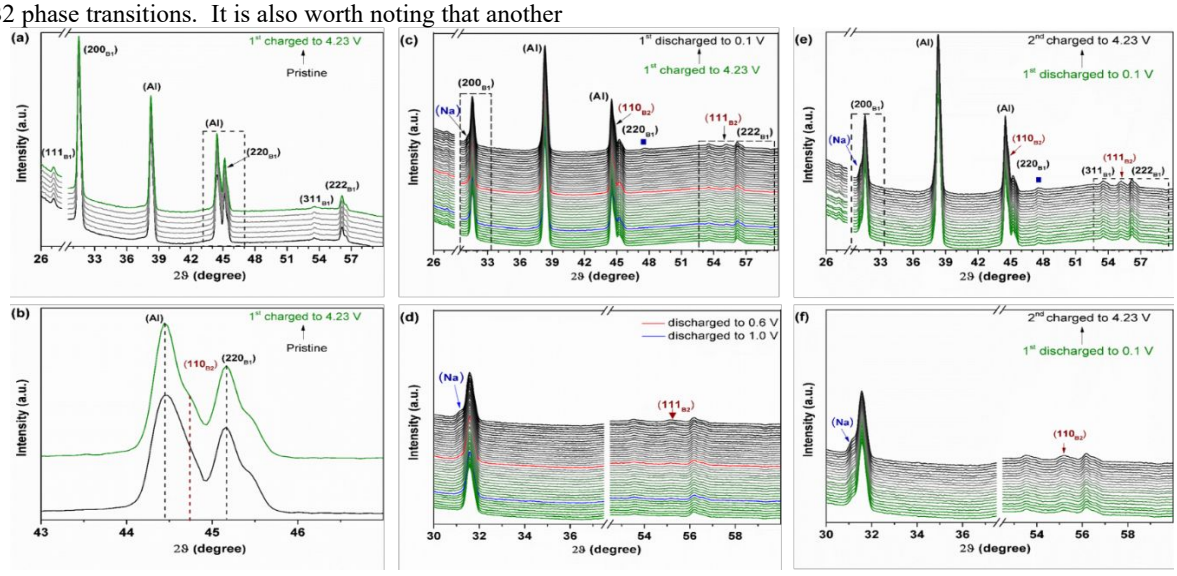

Figure 3. *In-situ* XRD study of sodium chloride electrode. (a, b) All *in-situ* XRD patterns for the 1st charge process with detailed patterns between 43° to 47°. Peak around 44.7° indicates partial phase transition of B1-type NaCl to B2-type NaCl. (c) *In-situ* XRD

patterns for the 1st discharge process. (d) Appearance of Na and (111) $_{B2}$ peaks around 31.2° and 55.2° indicate intercalation of sodium-ions and further B1 to B2 phase transition. (e, f) *In-situ* XRD patterns for the 2nd charge process showing downward shift of Na peak, during deintercalation of sodium-ions. In situ XRD patterns for 1st discharge and 2nd charge process are plotted by step of 5. The patterns of the sample were collected as ~5 min for each XRD scan). (: an unknown peak).

its relaxed state (Supplementary Figure 6), GITT experiment also proves that successive B1 to B2 phase transition decrease the polarization and provide easier electronic transfer.[24]

To elucidate the stoichiometries of materials, after employing the sodium intercalation/deintercalation mechanism, transmission electron microscopy-energy dispersive X-ray spectroscopy (TEM-EDS) was conducted as shown in Figure 4. Images and TEM-EDS patterns of the particles for the pristine (Figure 4a and 4b), fully discharged (Figure 4c and 4d), and charged (Figure 4e and 4f) NaCl-electrode were investigated. Na and Cl contents in fully discharged electrode were 61.3 and 38.7 at. %, respectively, which is different from the pristine electrode of 45.7 and 54.3 at. %. Hence, sodium content increased after intercalation of sodium-ions during discharge process. A TEM image of the electrode after the second charging (Figure 4e and 4f) reveals that Na and Cl contents are 52 and 48 at. %, respectively. This decrease in sodium peak is due to deintercalation of sodium-ions during charge process. The EDS elemental mapping of discharged electrode (Figure 4g) demonstrates that NaCl particles are covered by Na_2CO_3, NaF and $NaClO_4$ containing SEI layer (Supplementary Figure 7).[19,20] The SEI layer does not seem to exist in the fully charged electrode (after charged to 4.23 V), possibly because of the partial decomposition of the SEI layer components at high voltage. Doubaji *et al.* also explained that a thin layer of Na_2CO_3 and NaF covers the pristine electrode and reversible dissolution/reformation of these compounds is observed in initial cycles.[20] Although TEM observation for alkali halides has been limited, since they are vulnerable to the strong electron beam (Supplementary Note. 2 and Figure 8), as explained by Allen *et al.*[25] EDS spectra of fully charged and discharged electrodes demonstrate the formation of sodium-enriched Na_xCl: x>1compounds after intercalation of sodium-ions in the host structure.

The electronic interaction of ionic compound (Na^+Cl^-) with intercalated sodium-ions in sodium enriched Na_xCl: x>1compound and the irreversible capacity loss in the initial cycles was further studied by X-ray photoelectron spectroscopy (XPS). Photoemission lines of carbon, fluorine, oxygen, chlorine, and sodium were measured to examine the consumption of sodium-ions during the discharge process. XPS spectra were measured for the pristine material and after the completion of first and second charge and discharge cycle (Figure 5). The XPS spectra for C 1s, Na 1s, F 1s, Cl 2p, and O 1s are shown in Figure 5 (a-f). In the C1s core level spectra (Figure 5a), the signature is mainly due to carbon black and PVDF. The main peak located at a binding energy of 284.5 eV is assigned to a C-C bond and corresponds to carbon black, which was used as an electronic conductive element in the electrode. The peaks at binding energies of 285.9 and 290.7 eV were assigned to the C-O and PVDF binder containing species. The two minor peaks at binding energies of 285.0 and 288.6 eV were assigned to hydrocarbon and -CO_2 related carbonaceous species, respectively, which usually exist at the outermost surface of the electrodes.[20,27] At the end of the first and second discharges, a peak at 289.5 eV appeared that corresponds to formation of a SEI layer containing Na_2CO_3 on the surface as a result of electrolyte reduction. Hence, consumption of sodium-ions is not limited to the formation of so sodium-enriched metallic compounds but also from the formation of carbonaceous and oxygenated species containing SEI layer on the electrode surface.

The evaluation of the SEI layer is further explained by the F 1s and O 1s spectra. The F 1s spectrum (Figure 5b) of the pristine electrode is mainly dominated by the signal from the PVDF binder at a binding energy of 687.7 eV. The smaller peak at a

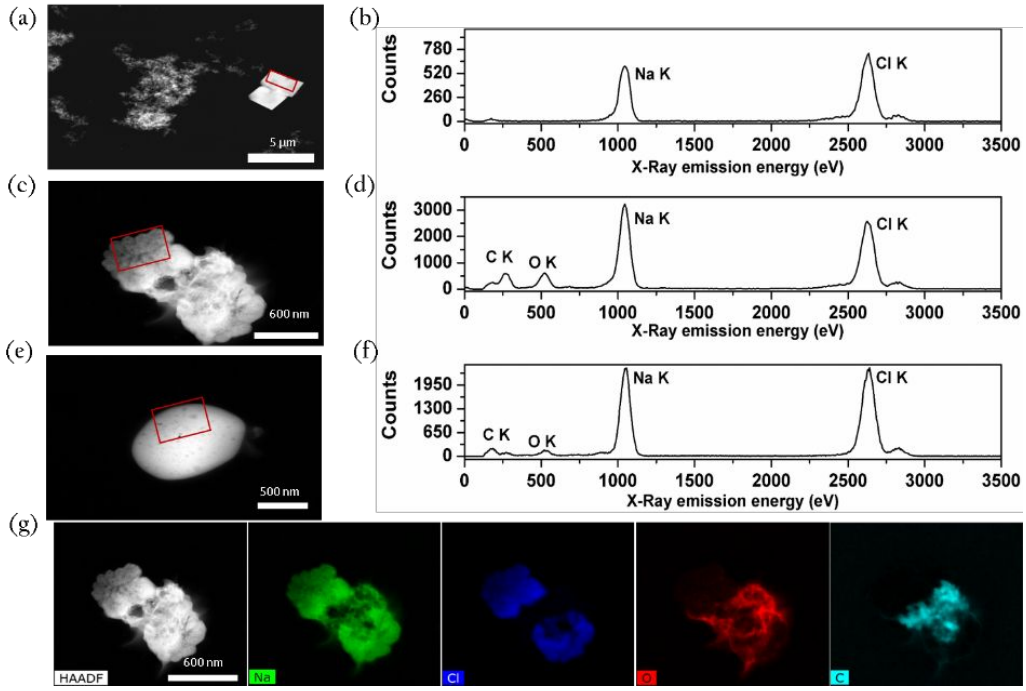

Figure 4. TEM-EDS analysis of NaCl. TEM images and EDS patterns of the (a, b) pristine, (c, d) fully discharged and (e, f) fully charged electrode. (g) High angle annular dark field image with TEM-EDS element mapping of sodium (Na), chlorine (Cl), oxygen (O) and carbon (C) for the fully discharged electrode.

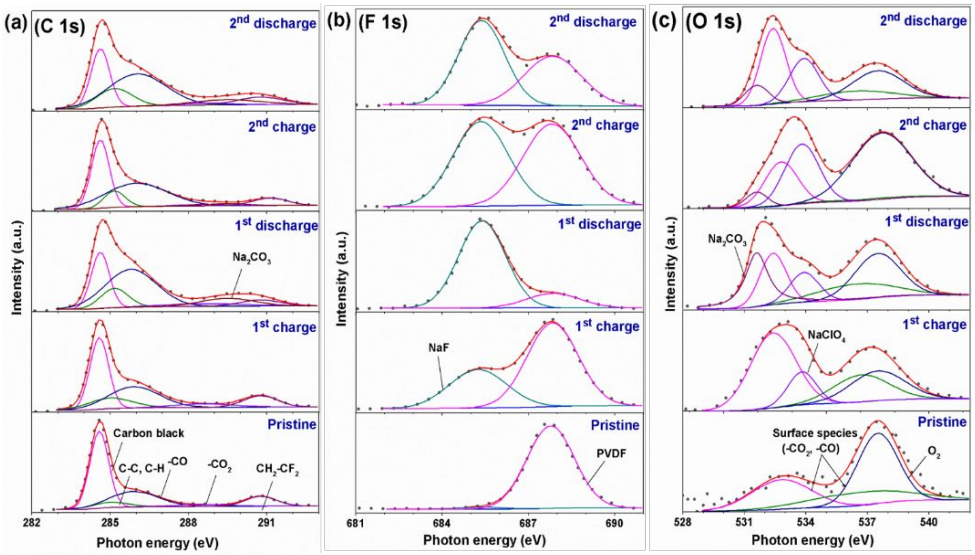

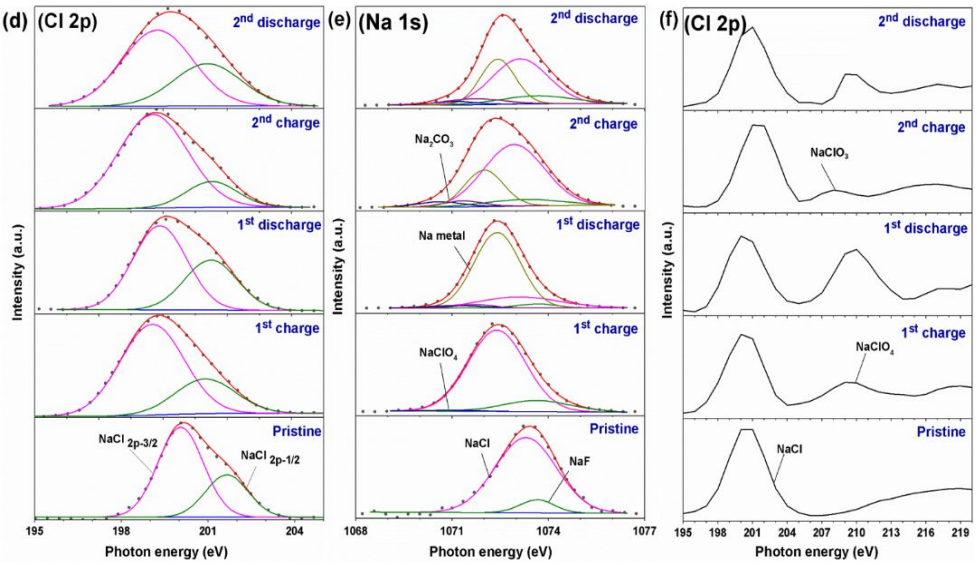

Figure 5. XPS surface study of NaCl electrode. XPS spectra of (a) carbon (C 1s), (b) fluorine (F 1s), (c) oxygen (O 1s), (d) chlorine (Cl 2p), (e) sodium (Na 1s) and (f) sodium perchlorate, sodium chlorate ($NaClO_4$, $NaClO_3$) for the pristine, fully charged and discharged electrodes during 1st and 2nd cycles. (Dotted and solid line (red) spectra represent the observed spectra and summation of peaks energies, respectively).

binding energy of 685.3 eV is present at the outermost surface and can be assigned to the formation of NaF due to the degradation of the binder during electrode preparation.[20] The increase in the intensity of NaF at the end of first and second discharges corresponds to the reduction of the electrolyte and formation of the SEI layer in the presence of the fluoroethylene carbonate (FEC) additive in the electrolyte. The O 1s core-level spectrum of the pristine electrode is shown in Figure 5c and has three distinct components. The peaks at binding energies of 532.4 and 536.7 eV are assigned to different oxygenated species at the surface. The peak at 537.5 eV can be seen in all spectra and might be due to the aggressive nature of NaCl toward moisture and air.[28] The appearance of the peak at a binding energy of 533.8 eV ($NaClO_4$) at the end of the first charge also confirms the decomposition of the electrolyte at higher voltages as shown in Figure 5f. Additionally, Cl_2 gas evolution is during a pre-charge step (Supplementary Figure 9). It shows that, in spite of deintercalation of sodium-ions during activation cycle (up to 4.3 V), there is no evolution of Cl_2. Therefore, the sodium-ion vacancies plays an important role for the B1- to B2- NaCl phase transition. In the fully discharged stage, a peak associated with Na_2CO_3 at 531.6 eV in Figure 5c appears. However, a decrease in the intensity of Na_2CO_3 and NaF peaks also confirms partial dissolution of the SEI layer at high voltage (4.23 V) during the charge process.

In this study, the evolution of the interaction of NaCl compound with intercalated metallic sodium, Na 1s and Cl 2p core-level spectra of the pristine and cycled electrodes are shown in Figure 5 (d-f). In the Cl 2p (Figure 5d) core peak spectra of NaCl, the two main peaks at binding energies of 200.0 and 201.6 eV (ΔV=1.6 eV) correspond to the Cl $2p_{3/2}$ and Cl $2p_{1/2}$ orbitals. The Na 1s spectrum (Figure 5e) confirmed the presence of NaF at the surface, and the main peak at a binding energy of 1073.3 eV corresponds to the NaCl phase. These Na 1s and Cl 2p spectra led to the following explanation; after the first charge, the main Na 1s and Cl 2p peaks (Figure 5d) shift toward lower energy levels due to deintercalation of sodium-ions. This decrease would reflect the weakening of some of the Na-Cl bonds due to a decrease in the positive or negative charge on sodium or chlorine, as explained by K. Kishi *et al.*[29] Additionally, in the spectra of the fully discharge electrode, an intense Na-peak (Figure 5e) appears that corresponds to the intercalation of sodium-ions in the NaCl structure. The NaCl peak in Na 1s spectra moved to a higher energy of 1073.1 eV. However, there is a difference of -0.2 eV from the initial binding energy value of 1073.3 eV in the pristine electrode, which might be due to increased number of electropositive sodium atoms in the coordination spheres of chlorine. In addition, the presence of Na-Na bonds is also accompanied by a weakening of the Na-Cl bonds and Cl $2p_{3/2}$ and Cl $2p_{1/2}$ peaks, (Figure 5d) which moved toward lower energies of 199.8 and 201.4 eV, respectively. Finally, at the end of the second charge, the main peak of NaCl returns to 1073.3 eV (Figure 5e), which confirms that any NaCl that was interacting strongly with Na-metal is now freed from the potential of the Na-metal crystal. The same phenomenon is also observed in the electrode during the second cycle, but the intensity of the metallized Na peak after the second discharge is weaker than that of the peak after the first discharge. This variation in the intensity of the Na peak also confirms the intercalation/deintercalation of sodium-ions through the host structure. A small peak at 1071.7 eV is also visible in the Na 1s spectrum (Figure 5e) that corresponds to the formation of Na_2CO_3. However, the $NaClO_4$ peak at 1071.1 eV (Figure 5e) and 209.5 eV (Figure 5f) that appears in the first charge step and is also observed in the O 1s spectrum confirms electrolyte decomposition at the electrode surface and formation of the SEI layer (Figure 5f). Hence, irreversibility in the initial cycles is due to formation of both sodium-enriched Na_xCl compounds and an SEI layer on the electrode surface. However, the SEI layer partially disappeared at the end of the charge (4.23 V) and

reappeared during the discharge process (0.1 V) as also explained by Doubaji *et al*.[20]

The evaluation of XRDs, XPS and TEM-EDS spectra clarified the formation of sodium-enriched Na_xCl: x>1, compounds through the electrochemical intercalation process of sodium-ions. Hence, to search for novel low-cost cathode materials for rechargeable NIBs, we studied the electrochemically induced phase transformation of B1-phase (Fm3m) to B2-phase (Pm3m) of sodium chloride and used this electrochemically metallized Na_xCl compound as a new cheap electrode material for NIBs. These results will contribute to the development of low cost rechargeable batteries from earth-abundant elements which are also operatable at room temperature.

The main component of table salt (or sea salt), sodium chloride, which is known to be an insulator with a high band gap at room temperature, is electrochemically metallized by electrochemically inducing Na-ion vacancies in the crystal structure. These vacancies cause a phase transition from B1- to B2-NaCl. This B2-NaCl is capable of intercalating sodium-ions and delivered a high discharge capacity of 267 mAh/g in the range of 0.1 to 4.23 V. A detailed study was conducted in order to explore the electrochemical performance and phase transition mechanism by EIS, CV, *ex-situ* and *in-situ* XRD analyses. This study shows that B1-NaCl is not electrochemically active; however, a phase transition to B2-NaCl not only reduces its charge-transfer resistance but also electrochemically activates the sodium chloride to intercalate sodium-ions during the discharge process and form a metallic phase with Na_xCl where x>1. To further confirm the extent of the charge compensation, XPS analysis was performed for the fully charged and discharged electrodes. This study shows distinctive Na-Na (metallic) and Na-Cl (ionic) bonding in the metallic-NaxCl (x>1) structure. XPS and TEM-EDS studies also confirmed the sodium-ion intercalation/deintercalation process and formation/dissolution of the SEI layer on the electrode surface during the cycling processes. This work suggests that various unexplored alkali halide intercalation systems can provide unlimited opportunities to design electrodes with better performance beyond that of conventional electrode materials used in rechargeable batteries.

Experimental Methods

Electrochemistry. NaCl (ACS reagent, >99%) was purchased from Sigma Aldrich. For the electrochemical tests, the electrodes were prepared by mixing NaCl, acetylene black, and polyvinylidene difluoride (PVDF) at an optimized ratio of 70:20:10. For fabricating acetylene black (AB) electrode, AB and PVDF are mixed at a ratio of 90:10. The slurry was cast onto aluminum foil and dried in an oven at 80 ℃. Subsequently, the electrodes were roll-pressed and dried under vacuum overnight at 80 ℃ before making the cells. The electrolyte used to make the coin cell (CR 2032) consists of 1 M $NaClO_4$ with PC: FEC (98:2). The cell fabrication was performed in an argon-filled glove box (Mbraun Unilab, Germany) with controlled contents of H_2O and O_2 below 0.1 ppm. Galvano-static measurements were conducted using a multichannel battery tester (Maccor 4000) in a voltage range of 0.1 V ~ 4.23 V at C-rates of 0.03 and 0.05.

Metallization of NaCl.

Metallization of NaCl was achieved by the following procedures. In the first step, vacancies are intentionally induced through the electrochemical pre-charge step up to 4.2 V (*i.e.,* the activation cycle), resulting a partial phase transition from B1- to B2-NaCl. Secondly, a discharge process to 0.1 V make sodium-ions to intercalate into this activated compound. During the discharge process, the electrochemically active B2-NaCl phase can effectively accommodate these sodium-ions and form a sodium-rich compound (Na_xCl, x >1).

Material characterization. *Ex-situ* XRD patterns were measured with a Dmax2500/PC (Rigaku, Japan) with Cu-Kα radiation (wavelength of 1.5418 Å). The XRD patterns were obtained with a scan speed of 0.02◦ per step over a 2θ range of 10-80◦. *In-situ* X-ray diffraction (XRD) measurements were performed using an R-AXIS IV++ Rigaku (in-house) with Mo-Kα radiation (wavelength of 0.7107 Å). PDXL integrated X-ray powder diffraction software was used to optimize the lattice parameters of crystal structures. The time-resolved X-ray diffraction (TR-XRD) patterns (~5 min for each XRD scan) of the samples were collected for charge and discharge process. For easy comparison, the 2θ values of the obtained spectra were converted to Cu-Kα radiation. To observe the phase transition in the *in-situ* precharging process, the slurry casting was kept thicker than that used for other XRD characterizations. For high resolution XRD analysis, the electrode material was scratched from the Al-foil and sealed into the capillary tube. The electrode materials were scratched from the Al-foil and sealed into the capillary tube to measure the XRD [UNIST-PAL crystallography 6D beam line, Pohang Accelerated Laboratory (PAL)].

EIS and CV tests were conducted with coin cells using a Biologic potentiostate/galvanostate model VMP3 (Bio Lab, Inc.) and CVs were carried out in the voltage range from 0.1 V ~ 4.23 V at a scan rate of 0.1 mV/s. A PHI 5000 Versa Probe (Ulvac-PHI) equipped with an Al-Kα (1486.6 eV) monochromator was used to observe the state and chemical composition of elements at the surface of the NaCl. Galvanostatic intermittent titration technique (GITT) and half-cell performance studies were performed at a multichannel battery tester (Maccor 4000) in a voltage range of 0.1 ~ 4.23 V. A C/20 current pulse was applied for 10 minutes in a voltage range of 0.1 ~ 4.23 V. The rest time between the pulses are 60 minute to get more accurate open circuit potential. The core-level spectra presented in this study were energy calibrated from the arbitrary C 1s core-level peak of PVDF at a binding energy of 284.6 eV. TEM-EDS (Talos F200X, FEI) was used to observe the NaCl particle morphology and the elemental mapping for the pristine, fully charged and discharged electrode. The sample preparation for XPS and TEM-EDS analyses were performed by disassembling the cells at their fully charged or discharged states. The electrodes were collected and thoroughly washed to remove any residual salts. To investigate gas evolution during the electrochemical test, we used the *in-situ* gas measurement using the DEMS. The DEMS measurement was composed of a mass spectrometer (MS) (HPR-20, Hiden Analytical) and a potentio-galvano-static (WonA Tech, WBCS 3000). The NaCl electrode is assembled into a meshed coin cell, and a carrier gas of argon was flowed at 16 cc min^{-1} onto the coin cell. Schematic illustrations of the crystal structures of NaCl were drawn using the program VESTA.

ASSOCIATED CONTENT

Supplementary. This material is available free of charge via the Internet at http://pubs.acs.org at DOI:

Details of phase transition in NaCl without activation cycle, electron beam damage effect on alkali halides, Galvano-static profile of acetylene black electrode, Nyquist plot of NaCl electrode, *ex-situ* XRD characterization for phase transition, GITT analysis of NaCl electrode, TEM-EDS pattern of solid electrolyte interface on the electrode, HR-TEM images showing electron beam damage effect on alkali halides, Gas evolution analysis of NaCl electrode.

AUTHOR INFORMATION

Corresponding Author

E-mail: kychung@kist.re.kr

Notes

The authors declare no competing financial interest

ACKNOWLEDGMENT

This work was supported by the Technology Development Program to Solve Climate Changes of the National Research Founda-tion (NRF) funded by the Ministry of Science & ICT(grant number: 2017M1A2A2044482). This work was also supported by the KIST Institutional Program (Project No. 2E29642).

REFERENCES

(1) Brown, J. M. Equation of state and its uses as a pressure gauge in high pressure research. *J. Appl. Phys.* **1999**, 86, 5801, doi: 10.1063/1.371596

(2) Zhang, W.; Oganov, A. R.; Goncharov, A.F.; Zhu, Q.; Boulfelfel, S. E.; Lyakhov, A. O.; Stavrou, E.; Somayazulu, M.; Prakapenka, V. B.; Konôpková, Z. Unexpected stable stoichiometries of sodium chloride. *Science*. **2013**, 342, 1502-1505, doi: 10.1126/science.1244989.

(3) Oganov, A. R.; Saleh, G. Alkali sub-halides: high-pressure stability and interplay between metallic and ionic bonds. *Phys. Chem. Chem. Phys*. **2016,** 18. 2840-2849, doi: 10.1039/C5CP06026E

(4) Barnett, R. N.; Cheng, H. P.; Hakkinen, H.; Landman, U. Studies of excess electron in sodium chloride clusters and of excess proton in water clusters. *J. Phys. Chem*. **1995**, 99, 7731-7753, doi: 10.1021/j100019a062.

(5) Hongxia, B.; Mingwen, Z.; Hongcai, Z.; Yanling, D. Unusual electronic and mechanical properties of sodium chloride at high pressure. *Phys. Lett. A.* **2016**, 380, 1556-1561, doi: 10.1016/j.phys-eta.2016.02.036.

(6) Feldman, J. L.; Klein, B. M.; Mehl, M. J.; Krakauer, H. Metallization pressure for NaCl in the B2 structure. *Phys. Rev. B.* **1990**, 42. 2752-2760, doi: 10.1103/PhysRevB.42.2752

(7) Bassett, W. A.; Takahashi, T.; Mao, H. K.; Weaver J. S. Pressure induced phase transformation in NaCl. *J. Appl. Phys.* **1968**, 39. 319-325, doi: 10.1063/1.1655752.

(8) Nga, Y. A.; ONG, C. L. Mechanism of pressure-induced polymorphic transition in NaCl. *Phys. Rev. B*. **1992**, 46, 10547, doi: 10.1103/PhysRevB.46.10547 .

(9) Rajagopal, G.; Barnett, R. N.; Landmann, U. Metallization of ionic clusters. *Phys. Rev. Lett.* **1991**, 67, 727-730, doi: 10.1103/PhysRevLett.67.727.

(10) Kinoshita, T.; Mashimo, T.; Kawamura, K. The mechanism and effects of defects in the B1 –B2 phase transition of KCL under high pressure: Molecular dynamics simulation. *J. Phys. Condens. Matter.* **2005**, 17, 1027-1035, doi: 10.1088/0953-8984/17/6/021.

(11) Devani, S.; Anwar, J. A molecular dynamics simulation study of the effects of defects on the transformation pressure of polymorphic phase transformations. *J. Chem. Phys*. **1996**, 105. 3215-3218, doi.org/10.1063/1.471837.

(12) Kubota, K.; Komaba, S. Review-Practical issues and future perspective for Na-ion batteries. *J. Electrochem. Soc.* **2015**, 162. A2538-A2550, doi: 10.1149/2.0151514jes.

(13) Berthelot, R.; Carlier, D.; Delmas, C. Electrochemical investigation of the P2– NaxCoO2 phase diagram. *Nat. Mater.* **2011**, 10. 74-80, doi: 10.1038/nmat2920.

(14) Vassilaras, P.; Ma, X.; Li, X.; Ceder, G. Electrochemical properties of monoclinic NaNiO2 batteries and energy storage. *J. Electrochem. Soc.* **2013**, 160, A207, doi: 10.1149/2.023302jes.

(15) Ellis, B.L.; Nazar, L. F. Sodium and sodium–ion energy storage batteries. *Curr. Opin. Solid State Mater. Sci.* **2012**, 16, 168-177, doi: 10.1016/j.cossms.2012.04.002.

(16) Barpanda, P.; YE, T.; Nishimura, S. I.; Chung, S. C.; Yamada, y.; Okubu, M.; Zhou, H.; Yamada, A. Sodium iron pyrophosphate: A novel 3.0 V iron-based cathode for sodium–ion batteries. *Electrochem. Commun.* **2012**, 24, 116-119, doi: 10.1016/j.elecom.2012.08.028.

(17) Yabbuchi, N.; Kajiyama, M.; Iwatate, J.; Nishikawa, H.; Hitomi, S.; Okuyama, R.; Usui, R.; Yamada, Y.; & Komaba, S. P2-type Nax(Fe1/2Mn1/2)O2 made from earth-abundant element for rechargeable Na batteries. *Nat. Mater.* **2012**, 11,512-517, doi: 10.1038/nmat3309.

(18) Guo, S.; Li, Q.; Liu, P.; Chen, M.; Zhou, H. Environmental stable interface of layered oxides cathodes for sodium ion batteries. *Nat. Commun.* **2017**, 8, 1-9, doi: 10.1038/s41467-017-00157-8.

(19) Komaba, S.; Murata, T.; Ishikawa, T.; Yabuuchi, N.; Ozeki, T.; Nakayama, T.; Ogata, A.; Gotoh, K.; Fujiwara, K. Electrochemical Na insertion and solid electrolyte interphase for hard-carbon electrodes and application to Na-ion batteries. *Adv. Funct. Mater.* **2011**, 21, 3859-3867, doi: 10.1002/adfm.201100854.

(20) Doubaji, S.; Philippe, B.; Saadoune, I.; Gorgoi, M.; Gustafsson, T.; Solhy, A.; Valvo, M.; Rensmo, H.; Edström, K. Passivation layer and cathodic redox reactions in sodium-ion batteries probe be HAXPES. *ChemSusChem.* **2016**, 9, 97-108, doi: 10.1002/cssc.201501282.

(21) Komaba, S.; Ishikawa, T.; Yabuuchi, N.; Murata, W.; Ito A.; Ohsawa, Y. Fluorinated Ethylene Carbonate as Electrolyte Additive for Rechargeable Na Batteries. *ACS Appl. Mater. Interfaces,* **2011**, 3, 4165–4168, doi: 10.1021/am200973k.

(22) Ponrouch, A.; Dedryvère, R.; Monti, D.; Demet, A.E.; Ateba, J. M.; Croguennec, L.; Masquelier, C.; Johansson. P.; Palacín, M. R. Towards high energy density sodium ion batteries through electrolyte optimization. *Energy Environ. Sci.* **2013**, 6, 2361-2369, doi: 10.1039/C3EE41379A.

(23) Shin, H.; Park, J.; Sastry, A. M.; and Lu, W. Effect of fluoroethylene carbonate (FEC) on the anode and cathode interfaces at elevated temperature. *J. Electrochem. Soc.* **2015**, 162. A1683-A1692, doi: 10.1142/S0217984914500626.

(24) Naeem, U.; Murtaza, G.; Khenata, R.; Alahmed, Z. A.; Reshak, A. H. Phase transition, electronic and optical properties of NaCl under pressure. *Mod. Phys. Lett. B*. **2014**, 28, 14500621-14500629, doi: 10.1149/2.0071509jes.

(25) Bu, H.; Zhao, M.; Zhou, H.; Du, Y. Unusual electronic and mechanical properties of sodium chlorides at high pressure. *Phys. Lett. A.* **2016**, 380, 17, doi: 10.1016/j.physleta.2016.02.036.

(26) Allen, H. C.; Mecartney, M. L.; Hamminger, J. C. Minimizing transmission electron microscopy beam damage during the study of surface reactions on sodium chloride. *Microsc. Microanal.* **1998**, 4, 23-33, doi: 10.1017/S1431927698980023.

(27) Bodenes, L.; Darwiche, A.; Monconduit, L.; Martinez, H. The Solid Electrolyte Interphase a key parameter of the high performance of Sb in sodium-ion batteries: Comparative X-ray Photoelectron Spectroscopy study of Sb/Na-ion and Sb/Li-ion batteries. *J. Power Sources.***2015**, 273, 14-24, doi: 10.1016/j.jpowsour.2014.09.037.

(28) Gupta, D.; Kim, H.; Park, G.; Li, X.; Eom, H. J.; Ro, C. U. Hygroscopic properties of NaCl and NaNO3 mixtures particles as reacted inorganic sea salt aerosol surrogates. *Atoms. Chem. Phys.* **2015**, 15, 3379-3393, doi: 10.5194/acp-15-3379-2015.

(29) Kishi, K.; Kirimura, H.; Fujimoto, Y. XPS studies for NaCl deposited on the Ni (111) surface. *Surf. Sci.* **1987**, 181, 586-595, doi: 10.1016/0039-6028(87)90207-X.

Table of Contents